Planck intermediate results. XXV. The Andromeda Galaxy as seen by Planck

Michael Peel, Jodrell Bank Centre for Astrophysics, University of Manchester, *on behalf of the Planck Collaboration*

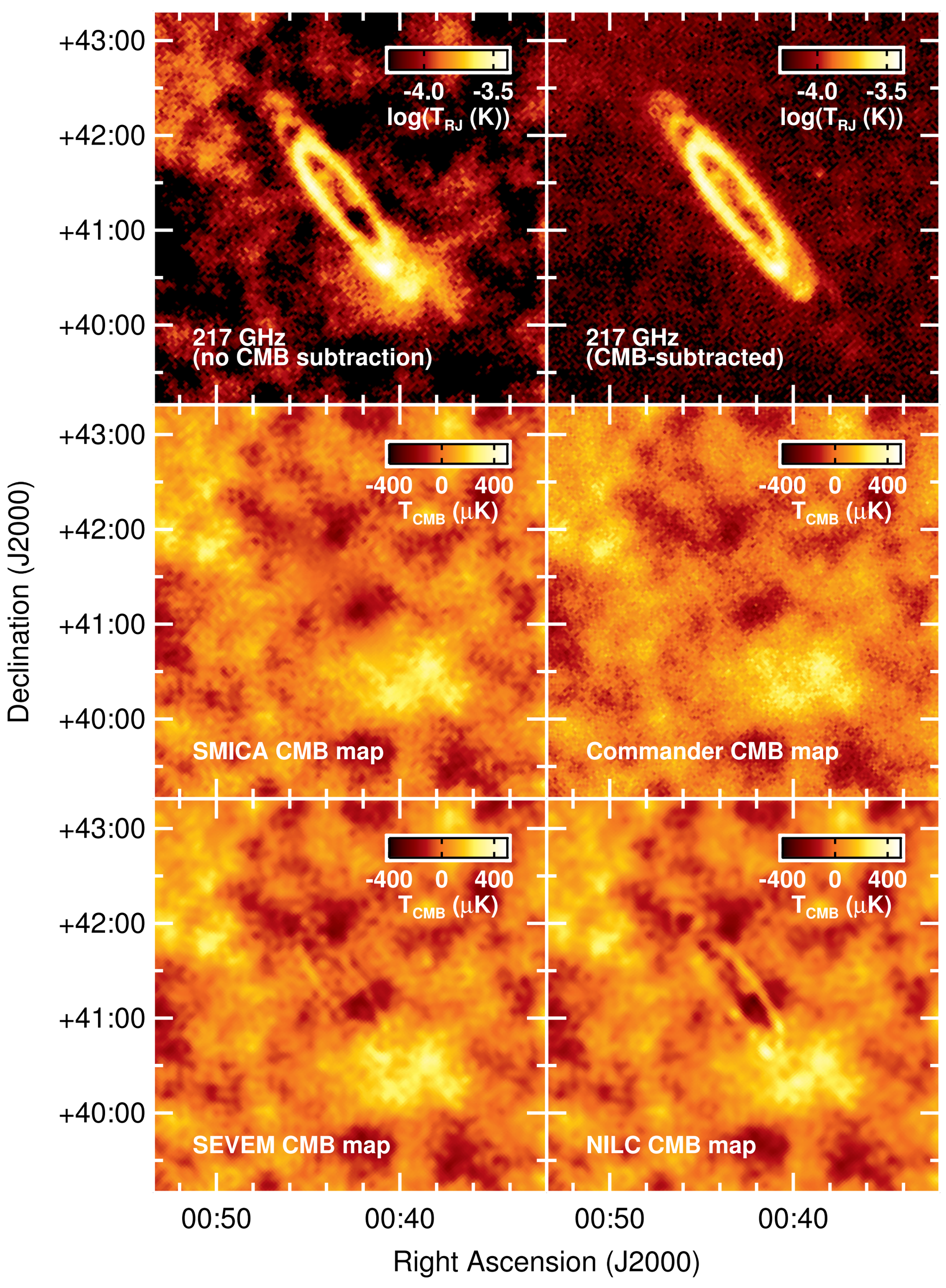

Fig. 1: Accurate CMB subtraction is important for M31.

The Andromeda Galaxy (M31) is one of a few galaxies that has sufficient angular size on the sky to be resolved by *Planck*. Accurate CMB subtraction is important given the similarities in angular scales between M31 and the CMB. Fig. 1 shows the different *Planck* CMB maps in the M31 region, and the best CMB-subtracted 217GHz map (using the SMICA CMB map).

Fig. 2 shows the CMB-subtracted *Planck* maps. A number of features are clearly visible in these, such as the outermost spiral arm structures at 545/857GHz (bottom-right of each panel), as well as NGC 205 and a bright background quasar.

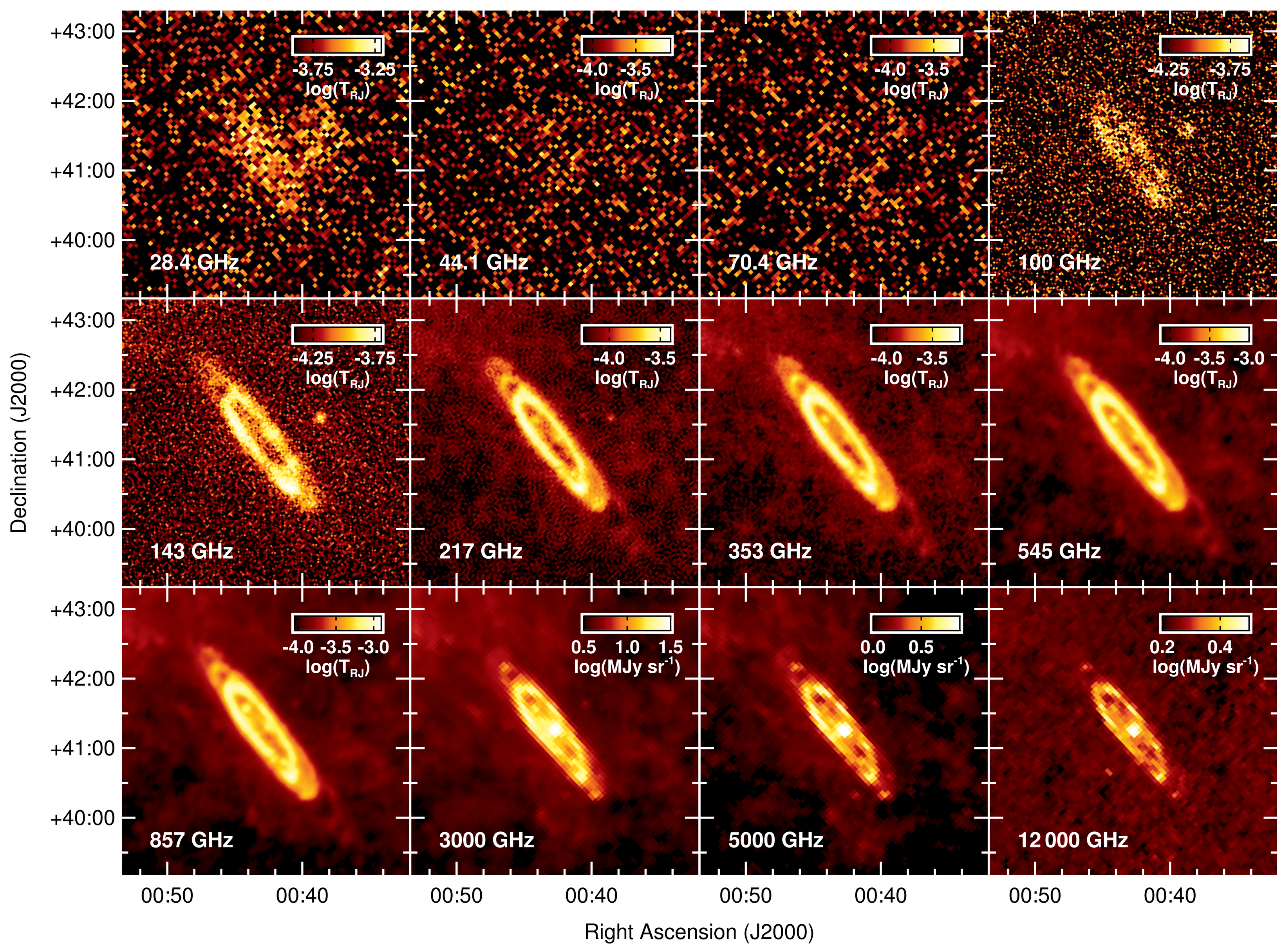

Fig. 2: CMB-subtracted maps at all *Planck* bands, plus 3 IRAS maps for comparison. *Planck* has detected M31 in all wavebands and clearly resolves multiple spiral arms and sub-features at >100GHz.

The integrated SED of M31, shown in Fig. 3, is well-fitted with a global dust temperature of 18.9 ± 0.9 K with a spectral index of 1.61 ± 0.11 and a significant amount of free-free emission at 20-60 GHz, which when converted into a star formation rate agrees well with the star formation estimate from Hα emission of 0.4 $M_\odot$ yr^{-1}. We see no evidence for spinning dust emission in the SED, with a 3σ upper limit of 1.26 Jy in the 20-60 GHz band, compared to the ~1 Jy expected from Galactic AME-100 μm ratios.

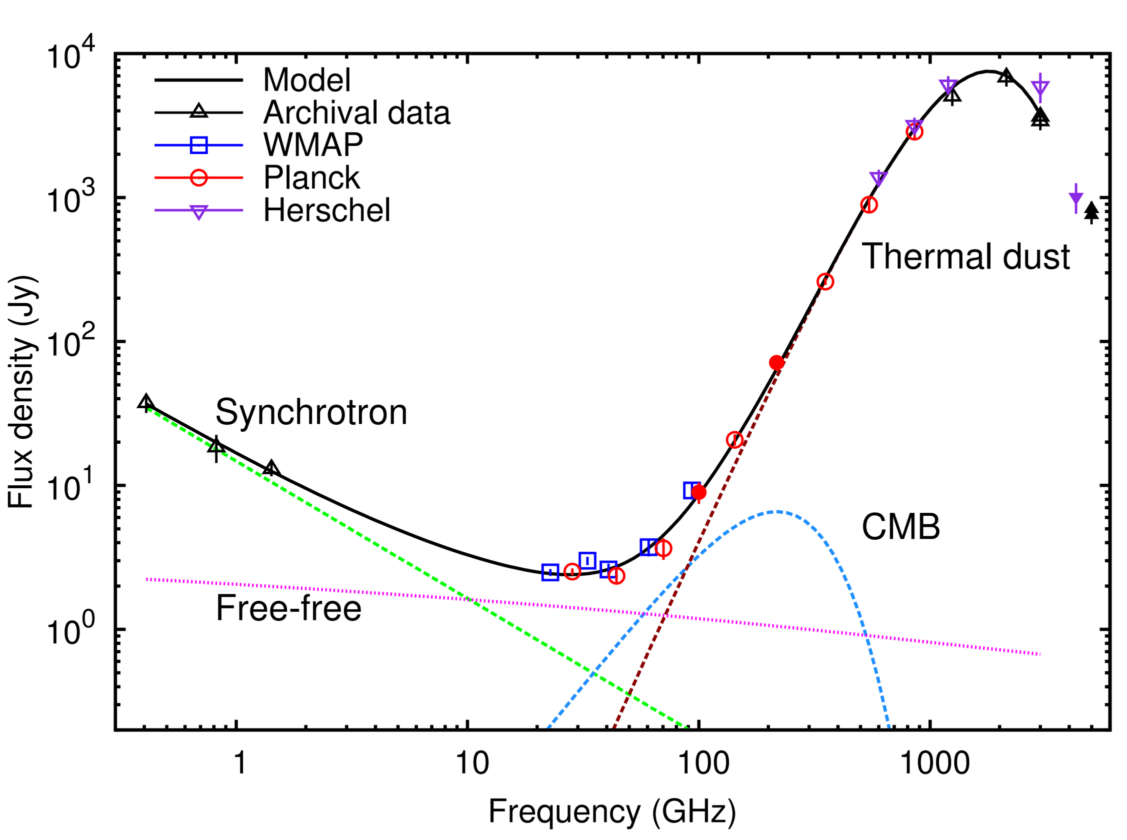

Fig. 3: The integrated SED of M31.

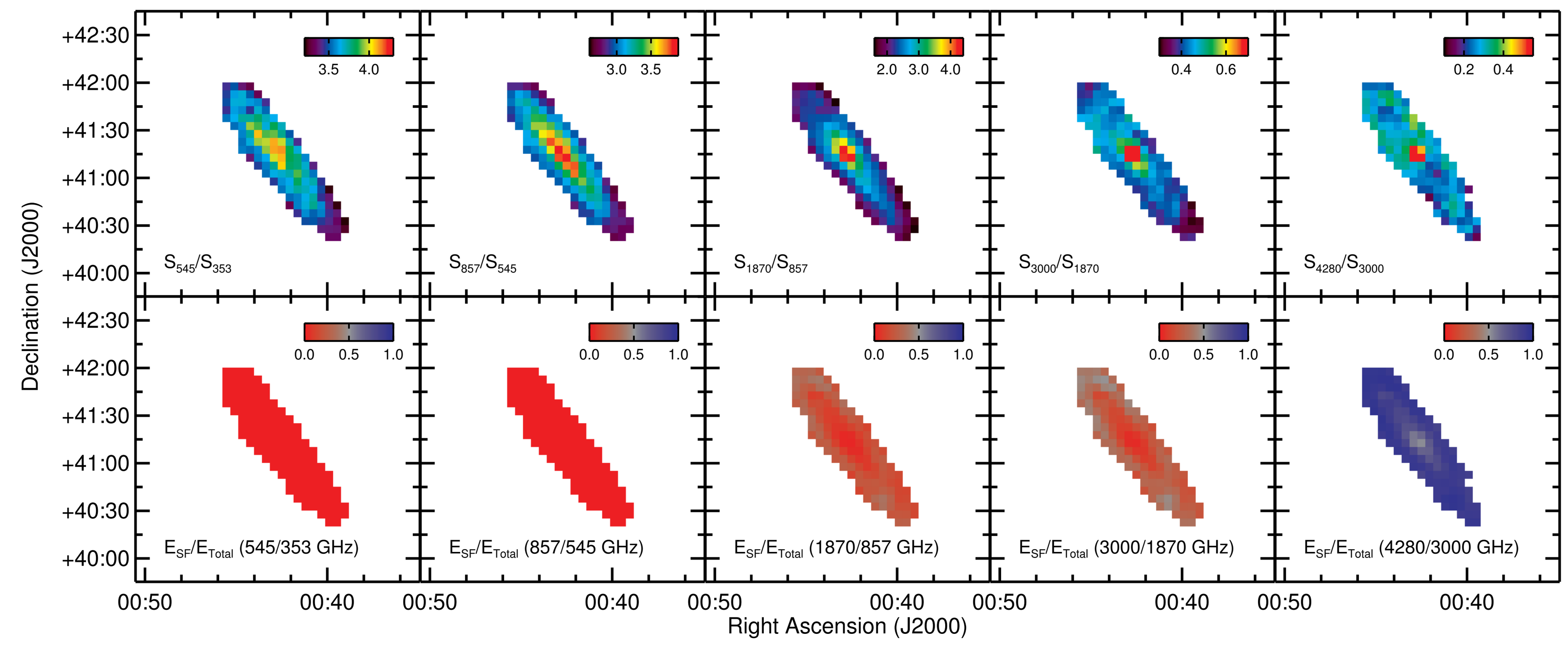

Fig. 4: Identifying the dust heating mechanisms.

We investigate the dust heating mechanism across M31. We find that dust dominating the longer wavelength emission (>0.3 mm) is heated by the diffuse stellar population (as traced by 3.6 μm emission), with the dust dominating the shorter wavelength emission heated by a mix of the old stellar population and star-forming regions (as traced by 24 μm emission). Fig. 4 shows the colour ratios for various bands (top row), and the fraction of the emission that is attributable to star formation in each colour ratio (bottom row); only the last ratio is dominated by the star-formation contribution.

We also fit spectral energy distributions (SEDs) for individual 5′ pixels and quantify the dust properties across the galaxy, taking into account the different heating mechanisms. Three examples of these are shown in Fig. 5; the top SED is for a pixel in the nuclear region of M31, the middle SED for a pixel on the northern edge of the 10 kpc ring; and the bottom picture for the bright pixel in the southern end of M31. The red points are the flux densities measured in the pixels; the blue points are the flux densities after rescaling using the colour ratios to only fit the cold dust contribution. In the nuclear region these two are the same; in the ring there is a difference between the two, which represents a decrease in temperature from 15.8 K to 14.3 K for the middle plot, and a 20 % increase in dust mass.

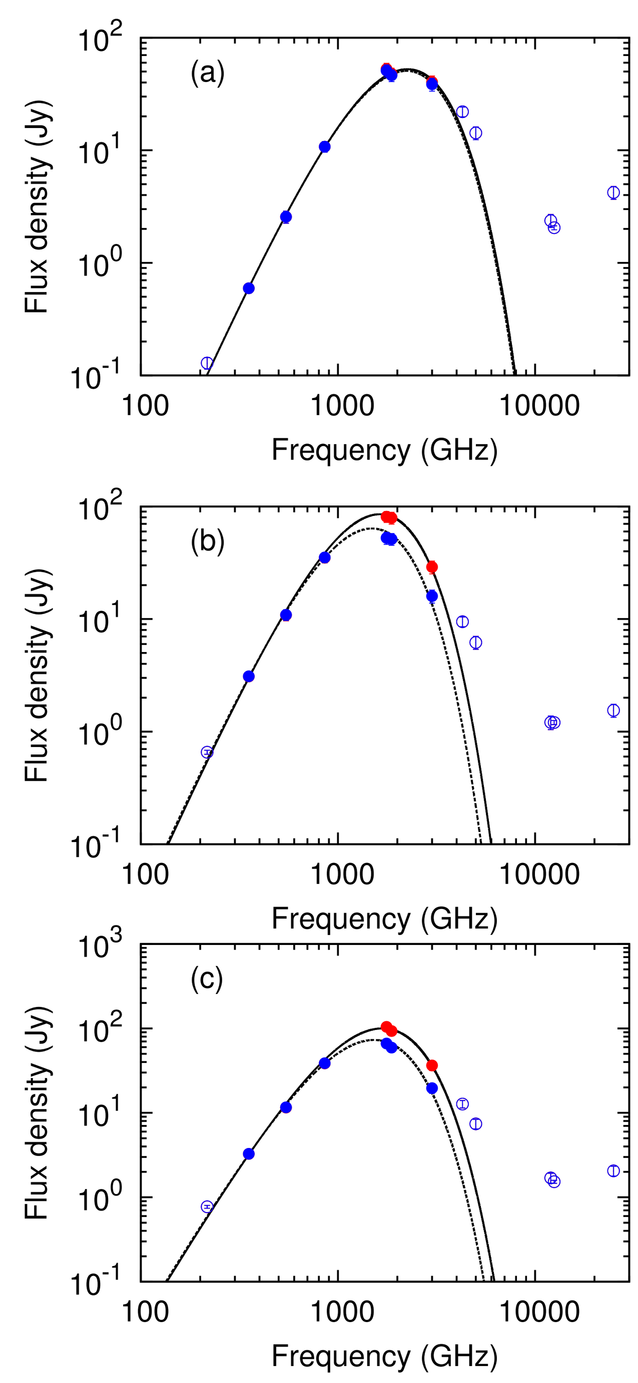

Fig. 5: SEDs of individual pixels.

The fitted dust parameters for the rescaled SEDs, fixing the spectral index to 2.0, are shown in map form in Fig. 6. We find that there is a linear decrease in temperature with galactocentric distance for dust heated by the old stellar population, as would be expected, with temperatures ranging from around 22 K in the nucleus to 14 K outside of the 10 kpc ring. We have also used a variable spectral index to fit the data, and find that the spectral index traces the heating from the old stellar population rather than measuring the dust grain properties.

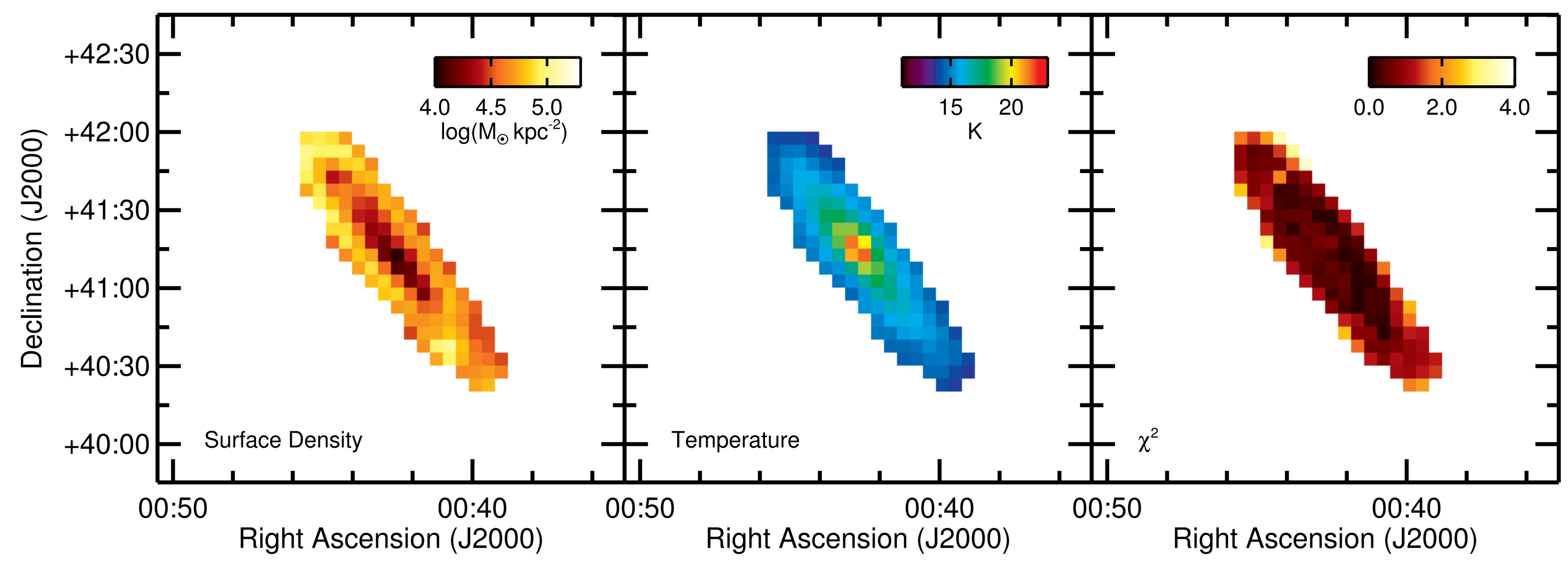

Fig. 6: Fitted dust parameters to the cold dust.

A&A (submitted), arXiv:1407.5452